Protein Expression and Purification 236 (2025) 106801

Contents lists available at ScienceDirect

Protein Expression and Purification

journal homepage: www.elsevier.com/locate/yprep

Research Article

Toward reproducible PETase research: A standardized workflow for reliable enzyme production and comparison

Katerina Jiraskova *, Jakub Ptacek, Kristyna Vydra Bousova, Jiri Vondrasek

Institute of Organic Chemistry and Biochemistry of the Czech Academy of Sciences, Flemingovo Namesti 2, 16000, Prague, Czech Republic

ARTICLE INFO

Keywords:
*Is*PETase
PET degradation
Enzyme activity assay
Optimization
Standardized protocol

ABSTRACT

The enzymatic degradation of polyethylene terephthalate (PET) by PETases has gained significant attention as a potential solution for plastic waste management. However, the absence of a standardized protocol for PETase production across studies presents a challenge for consistent enzyme characterization and activity comparison. Variations in production methods, including expression systems and purification techniques, may contribute to discrepancies in reported PETase activities. Here, we present the development of a unified protocol for the production of wild-type and engineered *Is*PETase variants. This protocol comprises standardized expression, purification, and quality control steps to ensure reproducibility and reliability. By enabling more accurate comparisons of PETase variants and addressing inconsistencies in PETase production, this approach facilitates collaborative efforts to advance plastic degradation technologies and lays the groundwork for accelerating research in enzymatic PET degradation and its applications in plastic waste management.

1. Introduction

Plastics have become an integral part of modern life due to their versatility, durability, and cost-effectiveness. Global production continues to rise annually, reaching 413.8 million tons manufactured in 2023, with polyethylene terephthalate (PET) accounting for approximately 6.2 % [1]. Due to its excellent physical and chemical properties, PET is widely used in various applications, including textile fibers, food packaging and beverage bottles [2]. However, its extensive use, combined with insufficient waste management and predicted lifespan of 25–50 years [3], has significantly contributed to pollution [4]. PET waste accumulation in landfills or as floating waste islands in oceans not only contributes to ecological damage but also leads to the formation of microplastics (MPs) - contaminants that pose serious threats to ecosystems and, eventually, to human health. MPs are present nearly everywhere on Earth [5] and can enter the human organism by ingestion, inhalation, and dermal contact [6], with the potential to translocate to various body sites [5,7–10]. Their association with several diseases [6,11,12] highlights concerns about their potential toxicity and long-term health effects.

A sustainable approach to mitigating this issue involves improving plastic recycling and reintegrating PET waste into the production cycle. Traditional methods, such as mechanical and chemical recycling, face limitations in efficiency and sustainability, often generating secondary pollutants [13,14]. Therefore, great interest has been attracted by the enzymatic depolymerization as an environmentally friendly alternative. As plastics accumulate in the biosphere, increasing evidence suggests that microbes are evolving enzymes and catabolic pathways to degrade synthetic polymers, utilizing them as carbon and energy sources [15–17]. Furthermore, enzymatic degradation into its monomers, terephthalic acid (TPA) and ethylene glycol (EG), also enables the re-synthesis of new PET with properties identical to virgin material [18]. By efficiently closing the loop on post-consumer PET waste, enzymatic recycling presents a sustainable solution that allows it to re-enter the economy as valuable raw material, preserving its economic value while reducing environmental impact.

Extensive research has been conducted on improving PETases, as naturally occurring PETases, such as those derived from *Ideonella sakaiensis*, exhibit only limited catalytic efficiency [15]. To fully harness their potential, PETases with enhanced thermostability, substrate specificity, and degradation rates have been developed through various rational engineering approaches [17,19–23]. Biocatalytic degradation has progressed from generating trace amounts of monomers after weeks of incubation to efficient depolymerization within several hours [24].

* Corresponding author.
E-mail addresses: katerina.jiraskova@uochb.cas.cz (K. Jiraskova), jakub.ptacek@uochb.cas.cz (J. Ptacek), kristyna.bousova@uochb.cas.cz (K. Vydra Bousova), jiri.vondrasek@uochb.cas.cz (J. Vondrasek).

https://doi.org/10.1016/j.pep.2025.106801
Received 30 June 2025; Received in revised form 11 August 2025; Accepted 13 August 2025
Available online 15 August 2025

Despite these advances, optimizing PET degrading enzymes for large-scale biotechnological applications remains a challenge and continues to be relevant and extensively studied topic.

A large number of studies have been conducted, however different research groups employed varying experimental conditions [24], making direct comparison of results very challenging. Key factors in protein production, such as expression organism, host strain, genetic sequences, or buffer composition can significantly impact protein yield, solubility, stability, and overall quality of the final protein [25,26]. Additionally, purification techniques such as Immobilized Metal Affinity Chromatography (IMAC) and Size Exclusion Chromatography (SEC), influence the purity and activity of the final protein. This methodological diversity adds to the challenges already posed by inconsistent assay conditions (e.g., PET substrate type, crystallinity, concentration, buffer composition, temperature, and pH) and further complicates the assessment and accurate comparison of enzyme performance.

In this study, we aim to provide a deeper understanding of PETase expression and purification conditions, and their potential impact on protein activity. Five *Is*PETase variants with distinct properties were produced and tested for PET degradation activity to support the development of a standardized protein production protocol. By implementing consistent production processes, we seek to improve reproducibility and reliability in PETase research. A unified approach will facilitate meaningful comparisons among different engineered variants and accelerate the development of efficient PET-degrading enzymes for industrial and environmental applications.

2. Materials and methods

2.1. Cloning

Genes encoding *I. sakaiensis* 201-F6 *Is*PETase (WT, GenBank GAP38373.1) and its mutants (W185A and W159H/238F) were a gift from Gregg Beckham & Christopher Johnson (Addgene plasmid # 112202; http://n2t.net/addgene:112202; RRID:Addgene_112202; Addgene plasmid # 112204; http://n2t.net/addgene:112204; RRID: Addgene_112204 and Addgene plasmid # 112203; http://n2t.net/addgene:112203; RRID:Addgene_112203) [17]. All variants were received in a form of pET21b(+) plasmid in *E. coli* DH5alpha growth strain as agar stab. Plasmid DNA was purified from an overnight liquid culture using High-Speed Plasmid Mini Kit (GeneAid, New Taipei City, Taiwan). The sequence of the extracted plasmid was verified by Sanger Sequencing performed by SEQme, Czech Republic.

The DNA sequences encoding variants of wild-type *Is*PETase - FAST_PETase [27] and HOT_PETase [22] - were synthetized, codon optimized for *E.coli* expression using a population-based evolutionary algorithm (commonly known as a Population Immune Algorithm), and cloned by GenScript (Rijswijk, Netherlands). The genes were inserted into pET21b(+) vector by extensions containing restriction endonuclease recognition sites: NdeI and XhoI for FAST PETase and BamHI and XhoI for HOT PETase. The constructs were validated for in-frame translation with the downstream 6xHis tag expressed from pET21b(+).

Each construct consists of 298 amino acids, including the original signal peptide sequence (first 27 residues) from *Is*PETase_WT at the N-terminus and a C-terminal hexa-histidine epitope tag. The nucleotide sequences and corresponding expressed amino acid sequences of the genes used in this study are provided in Supplementary Information, Fig. S1.

2.2. Protein production

2.2.1. Bacterial strains

In order to determine an efficient expression host, six different *E. coli* strains (BL21(DE3), 69450-M, Novagen; C41 (DE3), CMC0017, Sigma Aldrich; Origami B(DE3), 70837, Novagen; Rosetta-gami B(DE3), 71136, Novagen; SHuffle® T7 Express lysY, C3030J, NEB; BL21-CodonPlus (DE3)-RIL, 230245, Agilent; Table S1) were transformed with the FAST_PETase expression plasmid using a standard heat shock transformation protocol (42 °C, 45 s). Bacterial suspensions were plated on Luria-Bertani (LB) agar plates supplemented with antibiotics (100 μg/ml ampicillin) and cultivated overnight. Positive clones were used to inoculate 5 ml of antibiotics-supplemented LB media (100 μg/ml ampicillin – all strains; 34 μg/ml chloramphenicol for Rosetta-gami B (DE3), SHuffle® T7 Express lysY, and BL21-CodonPlus (DE3)-RIL; and 30 μg/ml kanamycin for Rosetta-gami B(DE3) and Origami B) which were cultivated overnight at 37 °C/190 rpm. The cells were then centrifuged at 1,200×*g* for 5 min and used to generate glycerol stocks stored at −80 °C for up to 3 months.

The described protocol was used to transform all other vectors encoding PETase variants into *Escherichia coli* BL21-CodonPlus (DE3)-RIL (230245, Agilent, USA) competent cells.

2.2.2. Protein expression optimization

For the assessment of different cell strains, glycerol stocks of all FAST_PETase-transformed strains were used to inoculate 5 ml of antibiotics-supplemented LB media (Table S1) and cultivated overnight at 37 °C, 190 rpm, in 20 ml glass culture tubes (P916150, P LAB a.s., Prague, Czech Republic) with polypropylene screw caps and rubber seals, using an orbital incubator shaker (ES-60, MIULab, Hangzhou, China). Subsequently, 100 μl of each overnight culture was used to inoculate 10 ml of fresh antibiotics-supplemented LB media, and all cultures were cultivated under identical conditions to an optical density at 600 nm (OD600) of at least 0.6 before induction with 0.5 mM isopropyl β-D-1-thiogalactopyranoside (IPTG). Induced cells were incubated overnight at 20 °C in orbital shaker (New Brunswick Innova 40R, M1299-0096, Eppendorf AG, Hamburg, Germany).

Samples were taken before induction and after overnight cultivation (~18 h). Harvested cells were centrifuged at 1,200×*g* for 20 min at 4 °C and resuspended in 500 μl of lysis buffer (50 mM Tris-HCl pH 7.5, 100 mM NaCl, and 1.75 μM lysozyme) per 1 ml of culture. Cells were treated with 0.1 mM phenylmethylsulfonyl fluoride (PMSF), sonicated for a total of 2 min using an UP200St ultrasonic generator (Hielscher Ultrasonics, Teltow, Germany) with 5-s pulses followed by 10-s pauses and centrifuged at 21,000×*g* for 20 min at 4 °C. Loading buffer was added to the supernatant and pellet fractions, which were then boiled for 10 min at 95 °C and analyzed by 12 % SDS-PAGE.

To evaluate the distribution of soluble and insoluble protein fractions across different expression conditions, glycerol stocks of *E. coli* BL21 (DE3) (69450-M, Novagen, USA) and BL21-CodonPlus(DE3)-RIL (230245, Agilent, USA) strains were cultivated in LB broth supplemented with ampicillin (30 μg/ml) and chloramphenicol (34 μg/ml, for the RIL strain only). Cultivations were performed under the same conditions as described above, using 20 ml glass culture tubes (P916150, P-LAB a.s., Prague, Czech Republic) shaken at 190 rpm. Expression was tested at 16 °C, 25 °C, and 37 °C using orbital incubator shakers: Innova S44i (16 °C, S44I330001, Eppendorf AG, Hamburg, Germany), New Brunswick Innova 40R (25 °C, M1299-0096, Eppendorf AG, Hamburg, Germany), and ES-60 (37 °C, MIULab, Hangzhou, China). Induction was initiated at OD600 values of 0.5 or 0.9. One milliliter of cultures was collected at key time points: before induction, 1 and 3 h post-induction, and after overnight cultivation (~16 h). Harvested cells were processed following the previously described protocol and the resulting samples were analyzed using SDS-PAGE.

2.2.3. Expression protocol

For large-scale production, *E. coli* BL21-CodonPlus (DE3)-RIL glycerol stocks carrying vectors encoding PETase variants were used to inoculate a starter culture of 5 ml antibiotics-supplemented LB media. The starter cultures were incubated overnight at 37 °C/190 rpm in 20 ml glass culture tubes (P916150, P LAB a.s., Prague, Czech Republic) using an orbital incubator shaker (ES-60, MIULab, Hangzhou, China). The overnight cultures were then diluted into a final volume of 1 l of LB

medium containing antibiotics in 2 l Erlenmeyer baffled cell culture flasks (I299841, P-LAB a.s., Prague, Czech Republic) and incubated at 37 °C and 190 rpm using an orbital incubator shaker (Innova S44i, S44I330001, Eppendorf AG, Hamburg, Germany). When the OD600 reached 0.5, the incubation temperature was reduced to 20 °C/160 rpm. Once the OD600 reached 0.8–1.0, protein expression was induced by adding IPTG to a final concentration of 0.5 mM. Cultivation continued at 20 °C/160 rpm for an additional 16–18 h. Cells were harvested by centrifugation at 2,500×*g* for 25 min at 4 °C, and the resulting bacterial pellets were resuspended in 40 ml of lysis buffer (per 1 l culture). The lysis buffer composition varied and included 1 × PBS or 50 mM Tris-HCl, 300 or 500 mM NaCl, 10 mM imidazole, pH 7.5, and 7 μM lysozyme. Resuspended pellets were stored at −20 °C for further processing.

2.3. Protein purification

2.3.1. His-tag affinity chromatography

The cell lysate was thawed and sonicated on ice for 30 min in the presence of 0.1 mM PMSF, with amplitude of 35 %, using 5-s pulses followed by 10-s pauses. After sonication, the lysate was centrifuged at 27,300×*g* for 1 h at 4 °C. To capture His-tagged proteins, 40 ml of supernatant containing the protein was applied to a column with approximately 4 ml of Chelating Sepharose™ Fast Flow resin (17057502, Cytiva, Marlborough, MA, USA), charged with Ni^{2+} ions and equilibrated with binding buffer (depending on the lysis buffer: 1 × PBS or 50 mM Tris-HCl, 300 or 500 mM NaCl, 10 mM imidazole, pH 7.5). The column was thoroughly washed with 400 ml of wash buffer: 1 × PBS or 50 mM Tris-HCl, 300 or 500 mM NaCl, 60 mM imidazole; pH 7.5. The target protein was eluted in 25 ml of elution buffer: 50 mM Tris-HCl, 500 mM NaCl, and 600 mM imidazole; pH 7.5. The eluted fractions were analyzed by SDS-PAGE on a 12 % gel. All fractions were merged, and the protein solution was split into two portions: one half was stored at 4 °C for short-term use, while the remaining sample was dialyzed overnight against buffer (50 mM Tris-HCl, 500 mM NaCl, pH 7.5) before being stored for further analysis.

2.3.2. HisTrap

Alternatively, the lysate supernatant was subjected to purification using HisTrap HP 1 ml column (17524701, Cytiva, Marlborough, USA) using an ÄKTA pure purification system. The process was performed under the following conditions: equilibration buffer consisting of 50 mM Tris-HCl (pH 7.5) and 300 mM NaCl; a sample volume of 10 ml; a loading flow rate of 1 ml/min; wash buffer composed of 50 mM Tris-HCl (pH 7.5), 300 mM NaCl, and either 0, 10 or 40 mM imidazole; and elution via a gradient from 0, 10 or 40–600 mM imidazole over 20 ml, with collection in 1 ml fractions. The presence of the PETase was confirmed by SDS-PAGE analysis and selected fractions were further purified by SEC.

2.3.3. Size exclusion chromatography

Protein samples were concentrated to approximately 0.8–2 mg/ml using the 50 ml, 10-kDa cut-off Amicon Ultra Centrifugal Filter device (EMD Millipore Corporation, Burlington, MA, USA) and further purified by SEC on a Superdex 75 Increase 10/300 GL column (29148721, Cytiva, Marlborough, MA, USA). Separation was performed in a buffer containing 50 mM Tris-HCl (pH 7.5) and 150 mM NaCl on the ÄKTA pure protein purification system (GE Healthcare, USA) at a flow rate of 0.8 ml/min. Fractions containing the protein were analyzed by SDS-PAGE and verified by mass spectrometry (MS). Protein concentrations were estimated using the absorbance at 280 nm in a standard spectrophotometer (NP80, Implen, Munich, Germany).

2.4. Activity assay

The enzymatic catalysis assay, performed as a proof of activity on real substrates, was conducted in a 2 ml polypropylene screw-cap microtube (2330-00, SSIbio, CA, USA) containing 5 mg of semi-crystalline PET powder with a maximum particle size of 300 μm (ES306000/1, Goodfellow, UK) in 500 μl of running buffer: 50 mM Tris-HCl and 150 mM NaCl, pH 7.5. The reaction was initiated by adding the enzyme to a final concentration of 500 nM and incubated at 30 °C, 40 °C, or 50 °C for 48 h in tightly capped microtubes on a Thermo Shaker MTH100 with a block cover (MIULab, Hangzhou, China) set to 900 rpm. Samples were prepared in triplicate, with negative controls including enzyme without substrate and substrate-only in running buffer.

Activity was determined by monitoring the increase in absorbance at 240 nm, corresponding to the accumulation of soluble aromatic products containing C=O bonds (e.g., bis- and mono(2-hydroxyethyl) terephthalic acid (BHET, MHET respectively) and TPA; $\varepsilon 240 = 13.8\ mM^{-1}\ cm^{-1}$) [28,29]. UV absorption spectra were monitored over 48 h using a NanoPhotometer NP80 (Implen, Munich, Germany) with a sample volume of 1 μl.

3. Results

3.1. PETase variant selection

Numerous studies on PET-degrading enzymes have employed diverse expression and purification protocols. To address this variability, we selected five *Is*PETase variants with distinct properties, including the number and position of mutations, melting temperatures, and degradation activities (Table S2), to establish a standardized protocol for functional protein production in *E. coli* optimized for activity assays.

3.2. Expression condition optimization

To investigate potential differences in performance across strains, we evaluated the expression of six *E. coli* strains, i.e. BL21(DE3), BL21-CodonPlus (DE3)-RIL, SHuffle® T7 Express lysY, Rosetta-gami B(DE3), Origami B(DE3), and C41 (DE3), which have been previously used in published studies on PETases [19,21,22,30,31]. By comparing these strains, we aimed to identify the most efficient host for soluble protein production while also standardizing expression protocols to improve the reproducibility of experimental results.

All cells were induced with 0.5 mM IPTG at an OD600 of at least 0.6 and incubated overnight at 20 °C. Samples were collected before induction and after ~18 h of cultivation. Expression analysis revealed no significant differences in protein yield or solubility among the tested *E. coli* strains (Fig. S2). Therefore, based on previous projects in our laboratory, we selected BL21 (DE3) and BL21-CodonPlus(DE3)-RIL strains as candidates for optimizing expression condition [32–34].

Small-scale expression tests were performed at three different temperatures (16 °C, 25 °C, and 37 °C), with induction initiated at OD600 values of 0.5 and 0.9. Protein production was analyzed at various time points: before induction (0 h) and after induction (1, 3, and ~16 h). Soluble and insoluble protein fractions were analyzed by SDS-PAGE analysis to assess expression levels. The results indicate that at 37 °C the target protein is predominantly found in the pellet fraction (Fig. S3A–D). At 25 °C, we observed an increase in the soluble fraction, which becomes visible on the gel as early as 3 h after induction (Fig. S3E–H). At 16 °C, soluble protein is also expressed; however, it is detectable on the gel only after overnight cultivation (Fig. S3I–L). Soluble protein was expressed at comparable levels in both strains at lower temperatures, however the highest production yield was achieved 16 h after induction at OD600 0.9 at 25 °C.

Based on both expression tests, we determined as standard conditions for large-scale protein production to be the BL21-CodonPlus(DE3)-RIL strain, with induction at an OD600 of 0.9, followed by overnight cultivation at 20 °C. SDS-PAGE analysis confirmed a satisfactory yield of soluble protein under these conditions (Fig. S4).

3.3. Protein purification

Hexahistidine-tagged proteins were purified from the soluble fractions of cell lysates. As a standard, we employed a two-step purification procedure consisting of gravity flow Ni-NTA affinity chromatography followed by SEC. The His_6-tag provided strong binding to the Ni-NTA agarose resin, allowing for efficient removal of protein impurities by washing with 60 mM imidazole. A band corresponding to PETase was observed on a Coomassie blue-stained SDS-PAGE gel after elution with a buffer containing a high concentration of imidazole (600 mM). The yield of protein obtained from Ni-NTA chromatography was consistent across different lysate buffer compositions. Washing with PBS buffer appeared to result in higher protein purity compared to Tris-HCl buffer, even when accounting for slightly higher enzyme loading in the latter condition (Fig. S5).

On the SEC column, PETase variants were eluted as a well-defined peak with maxima at approximately 13–14 ml. The purity of the final protein achieved through SEC remained consistent regardless of whether overnight dialysis was performed. Protein concentrations were estimated using calculated molar extinction coefficients based on absorbance at 280 nm. The final proteins exhibited very high purity, as demonstrated by SDS-PAGE with Coomassie blue staining (Fig. S6). PETase variants yielded milligrams of protein per liter of *E. coli* bacterial culture, with approximately 4 l of culture producing sufficient quantities of highly pure protein for detailed functional studies. Intact mass analysis of purified proteins confirmed the identity of PETase variants and the correct formation of all disulfide bridges present in the molecule. Additionally, it revealed the absence of the 27 N-terminal amino acids in all variants, demonstrating specific cleavage of the signal peptide during expression.

As an alternative purification method, we tested a commercially available HisTrap column, known for its stronger and more consistent binding. Our goal was to determine whether HisTrap alone could achieve results comparable to the standard two-step gravity flow Ni-NTA + SEC process. However, despite optimizing the HisTrap purification conditions by incorporating imidazole into the equilibration and wash buffers, the quality of the eluted protein remained lower compared to the Ni-NTA method (Fig. 1A–D). To achieve the desired purity level, SEC

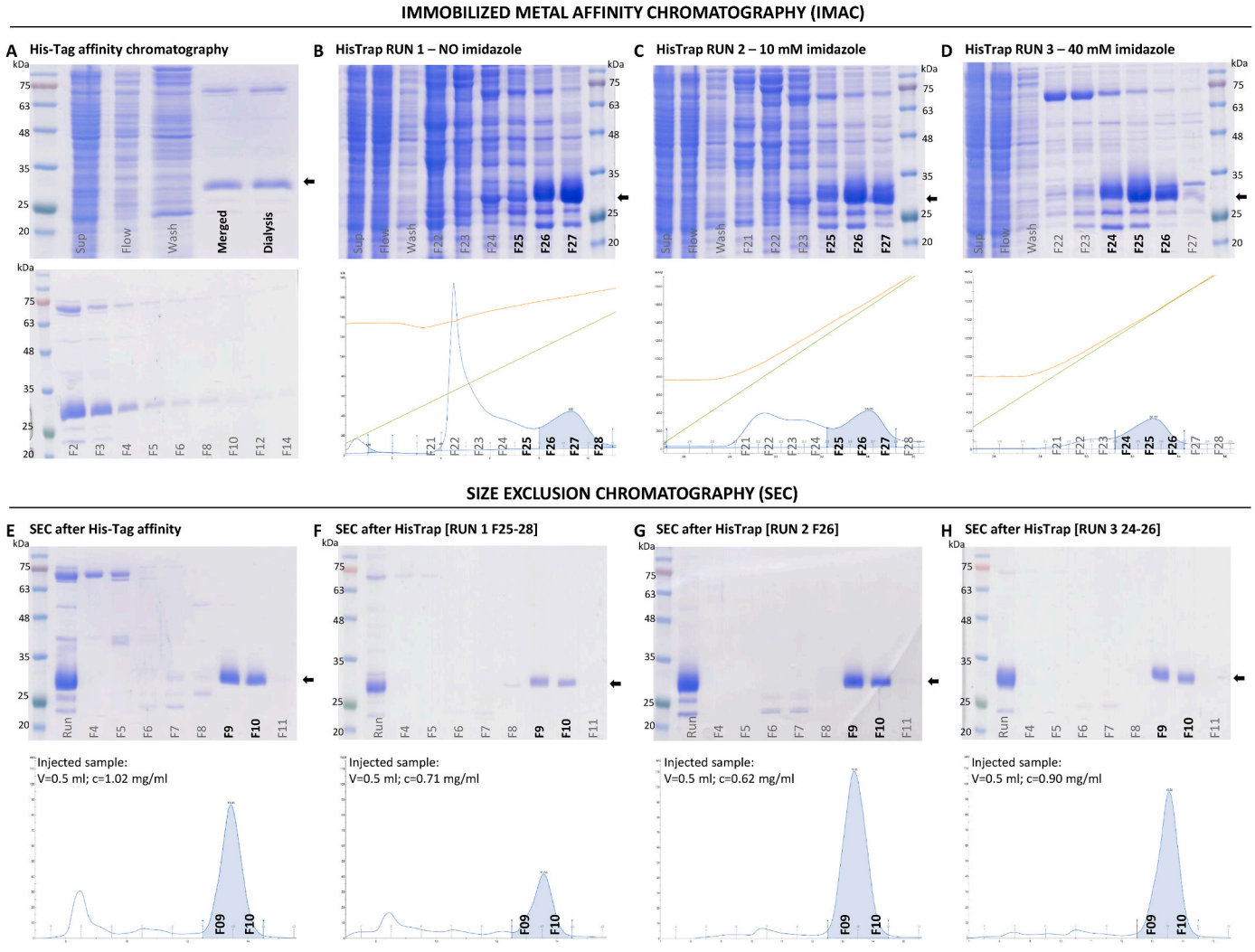

Fig. 1. Comparison of purification strategies using affinity and size exclusion chromatography. The cell lysate containing expressed FAST_PETase was divided into four 10 ml samples and purified using different affinity chromatography approaches: Ni-NTA (A) and HisTrap columns with varying imidazole concentrations (B–D). While Ni-NTA purification resulted in a highly pure eluate, HisTrap purification required optimization of imidazole levels to reduce non-specific binding. In the absence of imidazole (B), a substantial amount of contaminants was co-eluted, whereas increasing imidazole concentrations to 10 mM (C) and 40 mM (D) progressively improved protein purity. To further refine protein quality, all samples were subjected to SEC (E–H). SEC effectively removed remaining impurities, leading to comparable purity and yield across all purification methods. Lane labels include: Protein marker, Supernatant (Sup), Flow-through (Flow), Wash fraction, Purified fractions eluted with 600 mM imidazole (Merged), Purified fractions after dialysis (Dialysis), individual purified fractions(F), and injected sample applied to SEC (Run).

was employed as a second step, effectively removing residual contaminants and resulting in a final protein of comparable yield and quality to that obtained by the standard Ni-NTA + SEC workflow (Fig. 1E–H). Our results demonstrate that SEC serves as a crucial step in achieving consistent results, regardless of the initial affinity purification strategy.

3.4. Activity assay

Purified PETases were evaluated for their ability to hydrolyze PET using a spectrophotometric method that monitors absorbance at 240 nm, corresponding to the release of BHET, MHET and TPA over time. The hydrolysis of PET powder by the tested PETase variants was assessed at temperatures ranging from 30 °C to 50 °C for 48 h to determine their temperature-dependent activity.

Since different purification methods were used in this study, we examined whether specific steps influenced the final enzymatic activity. First, we investigated whether the removal of imidazole after IMAC affected the PET hydrolysis efficiency. A two-step purification approach using Ni-NTA affinity chromatography was performed, after which half of the eluted sample was dialyzed overnight, while the other half was directly subjected to SEC. The PET hydrolysis activity of FAST_PETase and HOT_PETase was then compared at 40 °C and 50 °C. The results showed that activity remained unchanged between dialyzed and non-dialyzed samples, with no measurable differences in degradation efficiency over the 24-h period (Fig. S7).

Next, we investigated the impact of the purification strategy itself on enzymatic performance. FAST_PETase 10 ml aliquots from identical lysate were processed using either a single-step IMAC approach (Ni-NTA or HisTrap) or a two-step method combining IMAC with SEC (Ni-NTA + SEC or HisTrap + SEC). PET hydrolysis activity was then evaluated for each purification method (Fig. 2). As expected, proteins purified using a single-step method exhibited significantly lower activity compared to a two-step method, likely due to lower sample purity, where only a small fraction of the total protein corresponds to the target enzyme. Furthermore, the higher enzymatic efficiency of the protein purified by Ni-NTA compared to HisTrap correlates with the greater purity achieved using this method. While activity differences between the two-step purification methods were less pronounced, they remained detectable despite the comparable final purity of both samples.

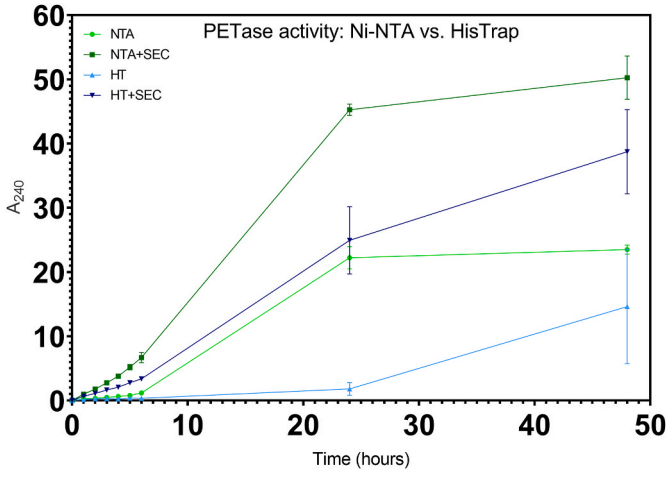

Fig. 2. Comparison of PET hydrolysis activity of proteins purified by different methods. PET hydrolysis activity was measured for FAST_PETase purified by different strategies: Ni-NTA (NTA, light green), Ni-NTA followed by SEC (NTA + SEC, dark green), HisTrap (HT, light blue), and HisTrap followed by SEC (HT + SEC, dark blue). All purification methods were performed using aliquots from the same cell lysate. Enzymatic activity was assessed at 40 °C by monitoring absorbance at 240 nm (A_{240}) over 48 h under standardized assay conditions: 5 mg PET powder, 500 nM enzyme, 0.5 mL running buffer (pH 7.5), and agitation at 900 rpm. Error bars represent standard deviations from triplicate measurements.

Finally, activity of all variants purified by Ni-NTA + SEC protocol was measured and compared. The wild-type variant displayed moderate activity at 30 °C, which declined with increasing temperature (Fig. 3A). The single mutant PETase_W185A exhibited low activity across all tested temperatures, confirming a detrimental effect of this mutation on catalytic efficiency (Fig. 3A). The double mutant PETase_W159H/238F showed moderate activity at 30 °C, which increased at 40 °C but was undetectable at 50 °C (Fig. 3B–C). In contrast, FAST_PETase remained catalytically active across all temperatures, with optimal hydrolysis observed at 40 °C. At 50 °C, a rapid initial phase of hydrolysis was followed by a plateau (Fig. 3B–D). HOT_PETase exhibited the highest activity at 50 °C, maintaining a steady hydrolysis rate over 48 h, while its activity at 40 °C is slightly lower but still significant (Fig. 3B–E). At 30 °C, all variants showed minimal degradation, further emphasizing the temperature dependence of enzymatic PET hydrolysis.

4. Discussion

Enzymatic hydrolysis has emerged as a promising strategy for addressing PET waste accumulation [35]. Since the discovery of *Ideonella sakaiensis* in 2016 [15], PETase has been extensively studied as the most suitable candidate for PET degradation. Initial research focused on structural analysis, for example, Austin et al. investigated the importance of active site residues, demonstrating reduced activity in the single-point mutation W185A [17]. Subsequent engineering efforts have focused on enhancing thermostability, increasing the melting temperature (T_m) toward the glass transition temperature (T_g) of PET (69–115 °C) [36]. At T_g, PET transitions from a rigid, crystalline state to a more flexible, amorphous form, enhancing polymer chain accessibility to PETase and significantly improving catalytic efficiency [24,37]. Notably, HOT_PETase achieved a T_m of up to 82.5 °C, demonstrating substantial progress in stability enhancement [22]. Despite these advancements, no PETase variant has yet achieved sufficient efficiency for large-scale applications, and research in this field remains highly active. A major challenge in PETase research is the significant variability in experimental protocols across studies, making direct comparisons difficult. The absence of a standardized production and testing protocol limits reproducibility and comparability, further hindering the identification of the most promising variants for optimization.

One of the first inconsistencies in published studies is the variation in expressed amino acid sequences. While some studies utilize the full-length sequence, including the 27-amino-acid N-terminal signal peptide [17,38,39], others employ a truncated variant where the N-terminus is removed [21,22,27,31,40]. To determine whether this sequence variation affects protein production or enzymatic PET degradation efficiency, we synthesized both full-length variants with the native signal peptide (FAST/HOT_PETase_LONG) and truncated versions (FAST/HOT_PETase_SHORT) to ensure all tested constructs were analogous and comparable. Expression tests showed that truncated variants repeatedly exhibited lower yield compared to their full-length counterparts (data not shown), highlighting the potential impact of N-terminal modifications on expression efficiency. However, intact mass analysis of the purified LONG variant revealed that the signal peptide is always cleaved, with a defined cleavage site resulting in a protein starting at Gln28 across all tested constructs. Therefore, the final proteins are equivalent to the SHORT variants, where the signal peptide is removed from the synthetic DNA, and the enzyme begins with Met, followed directly by Gln28. Since the signal peptide is naturally removed during expression, yielding a protein of the same length (neglecting the N-terminal methionine), its presence appears inconsequential for downstream applications and enzymatic activity.

The choice of expression system is another important factor influencing PETase production. While the majority of studies utilize *E. coli* as a host, various strains have been employed, each with distinct features affecting protein solubility, folding, and yield [19–22,30,31]. Our

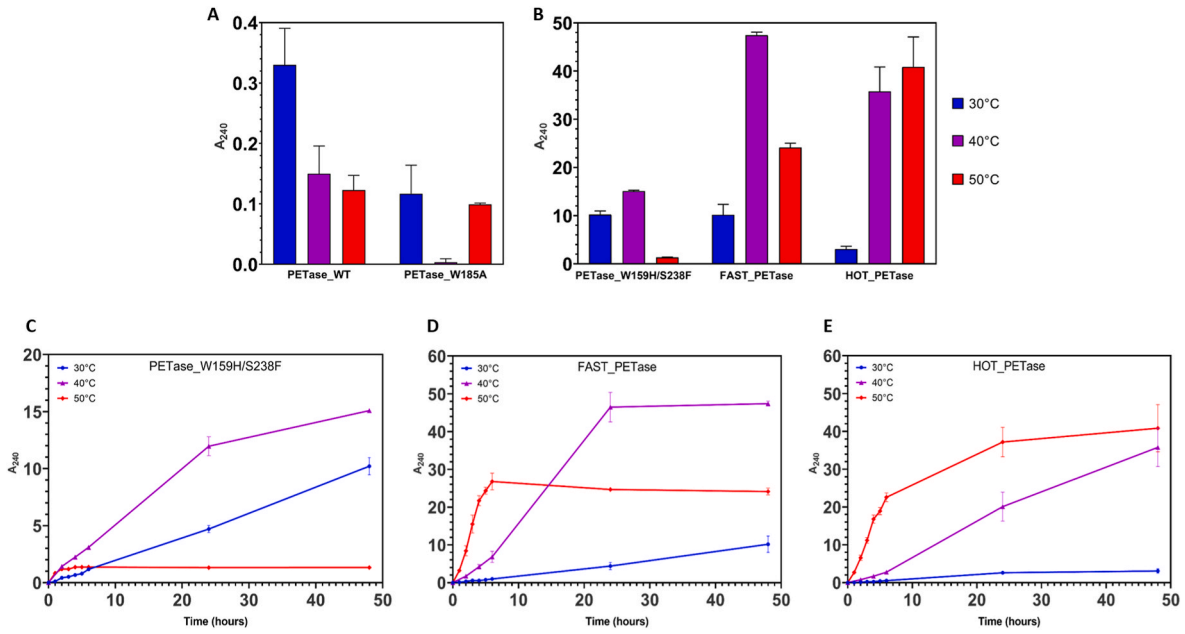

Fig. 3. PET hydrolysis by *Is*PETase variants. Purified PETase variants were evaluated for their ability to hydrolyze semi-crystalline PET powder (5 mg) in a standard assay format (500 nM enzyme, 0.5 mL of running buffer, pH 7.5) at three incubation temperatures (30 °C, 40 °C, and 50 °C) with a constant agitation at 900 rpm. PET degradation was monitored by measuring absorbance at 240 nm over 48 h. Measurements were performed in triplicate, with mean values and standard deviations reported. (A, B) Product release after 48 h: (A) Comparison of PETase_WT and PETase_W185A (B) PETase_W159H/S238F, FAST_PETase, and HOT_PETase. (C–E) Time-resolved PET hydrolysis kinetics at different temperatures (30 °C: blue, filled circles; 40 °C: purple, filled triangles; 50 °C: red, filled diamonds): (C) PETase_W159H/S238F (D) FAST_PETase (E) HOT_PETase.

evaluation of six different *E. coli* strains revealed no significant differences in protein solubility under standard expression conditions (~18 h of cultivation at 20 °C), suggesting that solubility alone may not be the primary determinant of strain selection. Instead, given that PETases contain four cysteine residues forming two disulfide bonds, and HOT_PETase has an additional third disulfide bond along with a free cysteine, selecting an *E. coli* strain optimized for disulfide bond formation is a logical consideration. Strains such as Rosetta-gami B(DE3), SHuffle® T7 Express, and Origami B(DE3) are commonly used for this purpose, as they facilitate proper protein folding in the reducing environment of the *E. coli* cytoplasm. While several studies have employed these strains for PETase expression [19,22,30,38,40,41], few have reported actual protein yield, making it difficult to determine whether their selection offers any advantage in production efficiency. A recent study by Carter et al. [26] compared the soluble production of PETase variants in multiple *E. coli* strains, finding that *Is*PETase_WT was optimally produced in SHuffle® T7 Express, whereas FAST_PETase and HOT_PETase achieved higher yields in BL21(DE3). However, despite these differences in expression levels, the PET-degrading activity remained within the expected range based on published studies for enzymes produced in either strain. Additionally, our MS results indicate correct formation of disulfide bridges even in the standard BL21(DE3) strain, suggesting that the ability to promote disulfide bond formation is not the key determinant in strain selection either.

Further optimization of expression parameters in our study confirmed that temperature and induction time play a crucial role in maximizing soluble protein yield. Expression at 37 °C predominantly led to accumulation of protein in the pellet fraction, whereas a lower induction temperature (20–25 °C) significantly improved the yield of soluble PETase. These results align with previous studies emphasizing that lower expression temperatures promote correct protein folding and reduce aggregation [24,37], indicating that expression conditions have a greater impact on protein yield than strain selection. To further increase production levels, bioreactor-based expression could be utilized [26]. Nonetheless, our optimized approach produced sufficient quantities of high-purity protein for detailed functional studies.

While IMAC is widely used for PETase purification, the choice of resin and buffer conditions differs across studies. We compared two common IMAC methods: gravity-flow Ni-NTA purification and HisTrap column purification on an ÄKTA system and found that Ni-NTA was more effective in obtaining high-purity PETase, whereas HisTrap exhibited more contamination even after imidazole optimization. Although HisTrap is sometimes used as a single-step purification approach, our results indicate that this method alone is insufficient for achieving high-purity protein. However, when combined with an additional SEC purification step following IMAC, residual contaminants were effectively removed, resulting in proteins of equivalent purity across both purification methods, despite a possible limitation arising from differences in buffer composition between the two IMAC protocols (e.g., NaCl concentration in the elution buffer).

Activity comparisons further confirmed the necessity of a two-step purification approach for standardized enzymatic assays. Proteins purified using Ni-NTA + SEC or HisTrap + SEC exhibited significantly higher specific activity than those obtained through single-step IMAC. While differences between two-step methods were less pronounced, Ni-NTA + SEC resulted in slightly higher activity, despite similar expected final protein purity. This suggests that while SEC effectively removes contaminants and improves protein quality, the initial IMAC step still influences overall enzymatic efficiency. Meanwhile, testing the impact of residual imidazole on protein activity revealed no significant differences, suggesting that imidazole does not impair catalytic function and that dialysis may not be necessary, thereby simplifying the workflow for future studies.

To validate our standardized Ni-NTA + SEC protocol, we assessed the activity of five *Is*PETase variants. The results correlate with the melting temperatures of individual variants. *Is*PETase_WT and PETase_W185A exhibited the highest activity at 30 °C but were severely compromised at temperatures above 40 °C, consistent with their low thermostability (T_m 45.1 °C) [30]. Similarly, the PET hydrolysis rate of PETase_W159H/238F increased at 40 °C but was undetectable at 50 °C, reflecting its improved but still limited thermostability (T_m 56.5 °C) [17]. FAST_PETase and HOT_PETase displayed significantly enhanced

hydrolysis rates at higher temperatures, in alignment with their greater thermostability (T_m 67.1 °C and T_m 82.5 °C, respectively) [22,27]. The time-dependent trends in enzyme activity further align with prior published data, highlighting the superior performance of engineered variants compared to wild-type enzyme [24].

While our work primarily addresses variability introduced during protein production, it is important to note that assay setup can also significantly affect observed activity. Parameters such as substrate type, enzyme-to-substrate ratio, running buffer volume, composition, pH, reaction temperature, and measurement intervals can all influence outcomes. Additionally, differences in evaluation methods—with some studies assessing % crystallinity change [17], others measuring aromatic product release via spectrophotometry [42], and some using HPLC-based quantification—introduce further variability. Some studies quantify aromatic products (TPA/MHET/BHET) separately [26], others combine TPA/MHET [19,22,27], or report all products together [21,30,38]. Therefore, to achieve reliable and comparable performance data across PETase variants, it is essential to use a consistent assay setup alongside standardized protein production.

Our results show that variability introduced during expression and purification may be an overlooked contributor to inconsistencies in PETase performance data. By addressing this upstream variability, we provide a foundation for unified methodologies and support broader standardization efforts in enzymatic PET degradation research.

5. Conclusions

This study establishes a standardized workflow for the expression and purification of *Is*PETase variants, addressing a critical barrier in PETase research: the lack of comparability between studies due to methodological variability. By benchmarking five *Is*PETase variants, including wild-type and engineered forms, the work demonstrates that expression conditions play a more significant role in soluble protein yield than strain selection, while purification approaches directly impact enzyme purity and performance.

The resulting protocol reduces inter-study variability and provides a robust, reproducible foundation for PETase performance assessment. This unified approach is a valuable contribution toward advancing the development of efficient biocatalysts for plastic waste biodegradation and upcycling.

CRediT authorship contribution statement

Katerina Jiraskova: Writing – original draft, Visualization, Validation, Methodology, Investigation, Conceptualization. **Jakub Ptacek:** Writing – review & editing, Validation, Methodology. **Kristyna Vydra Bousova:** Writing – review & editing. **Jiri Vondrasek:** Writing – review & editing, Supervision, Project administration, Funding acquisition, Conceptualization.

Declaration of generative AI and AI-assisted technologies in the Writing process

During the preparation of this work authors used ChatGPT 4o in order to improve the readability and language of the manuscript. After using this tool, authors reviewed and edited the content as needed and take full responsibility for the content of the published article.

Funding statement

This work has been financed by the Institute of Organic Chemistry and Biochemistry of the Czech Academy of Sciences (RVO: 61388963) and funded by the European Union under the Horizon Europe Programme, Grant Agreement No. 101082304 (BlueRemediomics). Views and opinions expressed are however those of the author(s) only and do not necessarily reflect those of the European Union or the European Research Executive Agency (REA). Neither the European Union nor the granting authority can be held responsible for them.

Conflict of interest statement

The authors declare that they have no conflicts of interest.

Appendix A. Supplementary data

Supplementary data to this article can be found online at https://doi.org/10.1016/j.pep.2025.106801.

Data availability

Data will be made available on request.

References

[1] PlasticsEurope, Plastics – the fast facts 2024: an analysis of European plastics production, demand and waste data [cited 2025 February]; Available from: https://plasticseurope.org/knowledge-hub/plastics-the-fast-facts-2024/.
[2] J. Schmidt, et al., Effect of Tris, MOPS, and phosphate buffers on the hydrolysis of polyethylene terephthalate films by polyester hydrolases, Febs Open Bio 6 (9) (2016) 919–927.
[3] F.G. Gallagher, Controlled degradation polyesters, in: J.a.L. Copolyesters, T. E. Scheirs (Eds.), Modern Polyesters: Chemistry and Technology of Polyesters, John Wiley & Sons, Chichester, UK, 2003, pp. 591–608.
[4] R. Geyer, J.R. Jambeck, K.L. Law, Production, use, and fate of all plastics ever made, Sci. Adv. 3 (7) (2017).
[5] Y.X. Yang, et al., Detection of various microplastics in patients undergoing cardiac surgery, Environ. Sci. Technol. 57 (30) (2023) 10911–10918.
[6] B. Zhao, et al., The potential toxicity of microplastics on human health, Sci. Total Environ. 912 (2024) 168946.
[7] H.A. Leslie, et al., Discovery and quantification of plastic particle pollution in human blood, Environ. Int. (2022) 163.
[8] L.C. Jenner, et al., Detection of microplastics in human lung tissue using μFTIR spectroscopy, Sci. Total Environ. (2022) 831.
[9] T. Horvatits, et al., Microplastics detected in cirrhotic liver tissue, EBioMedicine 82 (2022).
[10] L. Zhu, et al., Identification of microplastics in human placenta using laser direct infrared spectroscopy, Sci. Total Environ. 856 (Pt 1) (2023) 159060.
[11] R. Kumar, et al., Micro(nano)plastics pollution and human health: how plastics can induce carcinogenesis to humans? Chemosphere (2022) 298.
[12] R. Marfella, et al., Microplastics and nanoplastics in atheromas and cardiovascular events, N. Engl. J. Med. 390 (10) (2024) 900–910.
[13] F. Cao, et al., Research and progress of chemical depolymerization of waste PET and high-value application of its depolymerization products, RSC Adv. 12 (49) (2022) 31564–31576.
[14] Z.O.G. Schyns, M.P. Shaver, Mechanical recycling of packaging plastics: a review, Macromol. Rapid Commun. 42 (3) (2021) e2000415.
[15] S. Yoshida, et al., A bacterium that degrades and assimilates poly(ethylene terephthalate), Science 351 (6278) (2016) 1196–1199.
[16] B. Maheswaran, et al., In vivo degradation of polyethylene terephthalate using microbial isolates from plastic polluted environment, Chemosphere 310 (2023) 136757.
[17] H.P. Austin, et al., Characterization and engineering of a plastic-degrading aromatic polyesterase, Proc. Natl. Acad. Sci. U. S. A 115 (19) (2018) E4350–E4357.
[18] A. Maurya, A. Bhattacharya, S.K. Khare, Enzymatic remediation of polyethylene terephthalate (PET)-based polymers for effective management of plastic wastes: an overview, Front. Bioeng. Biotechnol. 8 (2020) 602325.
[19] S. Joo, et al., Structural insight into molecular mechanism of poly (ethylene terephthalate) degradation, Nat. Commun. 9 (2018).
[20] H.F. Son, et al., Structural bioinformatics-based protein engineering of thermostable PETase from Ideonella sakaiensis, Enzym. Microb. Technol. 141 (2020) 109656.
[21] Y.L. Cui, et al., Computational redesign of a PETase for plastic biodegradation under ambient condition by the GRAPE strategy, ACS Catal. 11 (3) (2021) 1340–1350.
[22] E.L. Bell, et al., Directed evolution of an efficient and thermostable PET depolymerase, Nat. Catal. 5 (8) (2022), 673-+.
[23] X. Ma, et al., Catalytic degradation of organophosphorous nerve agent simulants by polymer beads@graphene oxide with organophosphorus hydrolase-like activity based on rational design of functional bimetallic nuclear ligand, J. Hazard Mater. 355 (2018) 65–73.
[24] R. Wei, et al., Mechanism-based design of efficient PET hydrolases, ACS Catal. 12 (6) (2022) 3382–3396.
[25] J. Schmidt, et al., Effect of tris, MOPS, and phosphate buffers on the hydrolysis of polyethylene terephthalate films by polyester hydrolases, FEBS Open Bio 6 (9) (2016) 919–927.
[26] L.M. Carter, et al., Increased cytoplasmic expression of PETase enzymes in E. coli, Microb. Cell Fact. 23 (1) (2024) 319.

[27] H.Y. Lu, et al., Machine learning-aided engineering of hydrolases for PET depolymerization, Nature 604 (7907) (2022), 662-+.
[28] V. Pirillo, L. Pollegioni, G. Molla, Analytical methods for the investigation of enzyme-catalyzed degradation of polyethylene terephthalate, FEBS J. 288 (16) (2021) 4730–4745.
[29] V. Pirillo, et al., An efficient protein evolution workflow for the improvement of bacterial PET hydrolyzing enzymes, Int. J. Mol. Sci. 23 (1) (2022).
[30] S. Brott, et al., Engineering and evaluation of thermostable IsPETase variants for PET degradation, Eng. Life Sci. 22 (3–4) (2022) 192–203.
[31] X.X. Meng, et al., Protein engineering of stable PETase for PET plastic degradation by premuse, Int. J. Biol. Macromol. 180 (2021) 667–676.
[32] K. Bousova, et al., TRPM7 N-terminal region forms complexes with calcium binding proteins CaM and S100A1, Heliyon 7 (12) (2021) e08490.
[33] K. Bousova, et al., TRPM5 channel binds calcium-binding proteins calmodulin and S100A1, Biochemistry 61 (6) (2022) 413–423.
[34] V. Vetyskova, et al., Proteolytic profiles of two isoforms of human AMBN expressed in by MMP-20 and KLK-4 proteases, Heliyon 10 (2) (2024) e24564.
[35] F. Kawai, R. Iizuka, T. Kawabata, Engineered polyethylene terephthalate hydrolases: perspectives and limits, Appl. Microbiol. Biotechnol. 108 (1) (2024) 404.
[36] F. Awaja, D. Pavel, Recycling of PET, Eur. Polym. J. 41 (7) (2005) 1453–1477.
[37] N.A. Samak, et al., Recent advances in biocatalysts engineering for polyethylene terephthalate plastic waste green recycling, Environ. Int. 145 (2020) 106144.
[38] E. Erickson, et al., Comparative performance of PETase as a function of reaction conditions, substrate properties, and product accumulation, ChemSusChem 15 (1) (2022) e202102517.
[39] C. Waltmann, et al., Functional enzyme-polymer complexes, Proc. Natl. Acad. Sci. U. S. A. 119 (13) (2022) e2119509119.
[40] H.F. Son, et al., Rational protein engineering of thermo-stable PETase from for highly efficient PET degradation, ACS Catal. 9 (4) (2019) 3519–3526.
[41] E.Z.L. Zhong-Johnson, C.A. Voigt, A.J. Sinskey, An absorbance method for analysis of enzymatic degradation kinetics of poly(ethylene terephthalate) films, Sci. Rep. 11 (1) (2021) 928.
[42] T. Fecker, et al., Active site flexibility as a hallmark for efficient PET degradation by I. sakaiensis PETase, Biophys. J. 114 (6) (2018) 1302–1312.